Stamatoyannopoulos, G., Farquhar, M., Lindsley, D., Brice, M., Papayannopoulou, T., & Nuate, P. E. (1983) *Blood 61*, 530.
Stoeckert, C. J., Metherall, J. E., Yamakawa, M., Weissman, S. M., & Forget, B. M. (1987) *Mol. Cell. Biol. 7*, 2999.
Takihara, Y., Rutherford, T., Shiokawa, S., Fukumaki, Y., Endo, T., & Okano, H. (1987) *Leukemia 1*, 673.
van Assendelft, G. B., Hanscombe, O., Grosveld, F., & Greaves, D. R. (1989) *Cell 56*, 969.
Wei, C. M., Gibson, M., Spear, P. G., & Scolnick, E. M. (1981) *J. Virol. 39*, 935.
Wilson, J. T., Wilson, L. B., DeRiel, J. K., Villa-Komaroff, L., Efstratiadis, A., Forget, B., & Weissman, S. M. (1978) *Nucleic Acids Res. 5*, 563.
Wright, S., deBoer, E., Grosveld, F. G., & Flavell, R. (1983) *Nature 305*, 333.
Wright, S., Rosenthal, A., Flavell, R., & Grosveld, F. (1984) *Cell 38*, 265.

The Rate and Structural Consequences of Proline Cis–Trans Isomerization in Calbindin D_{9k}: NMR Studies of the Minor (*cis*-Pro43) Isoform and the Pro43Gly Mutant†

Johan Kördel,‡,§ Sture Forsén,§ Torbjörn Drakenberg,§ and Walter J. Chazin*,‡
Department of Molecular Biology, Research Institute of Scripps Clinic, La Jolla, California 92037, and Department of Physical Chemistry 2, Chemical Centre, University of Lund, S-221 00 Lund, Sweden
Received October 5, 1989; Revised Manuscript Received January 2, 1990

ABSTRACT: The EF-hand calcium-binding protein, calbindin D_{9k}, exists in solution in the calcium-loaded state, as a 1:3 equilibrium mixture of two isoforms, the result of cis–trans isomerism at the Gly42–Pro43 peptide bond [Chazin et al. (1989) *Proc. Natl. Acad. Sci. U.S.A. 86*, 2195–2198]. Nuclear magnetic resonance (NMR) studies of the minor (*cis*-Pro43) isoform and the Pro43 → Gly mutant are reported here. The rate of cis → trans isomerization at the Pro43 peptide bond in the wild-type protein was determined by line-shape analysis at elevated temperatures, using a sample in which all amino acids, except Ser and Val, were deuterated. The cis → trans rate is calculated to be 0.2 s^{-1} at 25 °C, corresponding to a free energy of activation, $\Delta G^{\ddagger}$, of 77 kJ/mol. The complete sequence-specific ^1H NMR assignments of the *cis*-Pro43 isoform and the Pro43 → Gly mutant in the calcium-loaded state have been obtained by using standard methods combined with comparisons to the previously assigned major (*trans*-Pro43) isoform. This has permitted detailed comparative analysis of ^1H NMR chemical shifts, backbone scalar coupling constants, and nuclear Overhauser effects. The minor isoform has a global fold that is identical with that of the major isoform. Structural changes imposed by cis–trans isomerization at Pro43 are highly localized to the linker loop (containing Pro43) that joins the two EF hands. The Pro43 → Gly mutant has a global fold that is identical with the wild-type protein, but does not exhibit conformational heterogeneity. Only very limited structural differences are observed between mutant and wild-type protein, and these are also highly localized to the linker loop. The ion-binding properties of the mutant, as determined by ^{43}Ca and ^{113}Cd NMR, are found to be very similar to the wild-type protein. These results provide crucial evidence that justifies the calculation of high-resolution three-dimensional structures of the Pro43Gly mutant, rather than of the conformationally heterogeneous wild-type protein.

Ca^{2+} ions play an important role in the regulation of a variety of cellular functions. This role is mediated by a class of highly homologous Ca^{2+}-binding proteins, the calmodulin superfamily (Kretsinger, 1987), that respond rapidly to transient increases in intracellular Ca^{2+} concentration. The mechanism of action for these proteins is believed to be based on marked conformational changes that are induced by Ca^{2+} binding. While knowledge about the details of the molecular structure has been obtained from the highly refined X-ray diffraction studies of parvalbumin (Moews & Kretsinger, 1975), calbindin D_{9k}[1] (Szebenyi & Moffat, 1986), calmodulin (Babu et al., 1988), and troponin C (Herzberg & James, 1988; Satyshur et al., 1988), in no case have crystals suitable for X-ray structure determination been obtained for *both* calcium-free and calcium-bound states of one of these proteins. Solution structure determination utilizing two-dimensional ^1H NMR[2] [reviewed in Wüthrich (1989)] is uniquely suited to overcome this problem.

† This work is supported by the National Institutes of Health (Grant GM 40120 to W.J.C.) and the Swedish Natural Science Research Council (graduate fellowship to J.K. and operating grants to S.F.).
* To whom correspondence should be addressed.
‡ Research Institute of Scripps Clinic.
§ University of Lund.

[1] Formerly the 9-kDa intestinal calcium binding protein (ICaBP).
[2] Abbreviations: 1D, one-dimensional; 2D, two-dimensional; COSY, correlated spectroscopy; 2QF-COSY, two quantum filtered COSY; DR-COSY, double relayed COSY; FID, free induction decay; NMR, nuclear magnetic resonance; NOE, nuclear Overhauser effect; NOESY, 2D NOE spectroscopy; Quin2, 2-[[2-[bis(carboxymethyl)amino]-5-methylphenoxy]methyl]-6-methoxy-8-[bis(carboxymethyl)amino]quinoline; r-calbindin, the minor A form of bovine calbindin D_{9k} with an additional methionine at the N-terminus, produced by recombinant DNA methodology; P43G, mutant of r-calbindin with Pro43 substituted by glycine; P20G, mutant with Pro20 substituted by glycine; N21Δ, mutant with Asn21 deleted.

0006-2960/90/0429-4400$02.50/0 © 1990 American Chemical Society

As a first step toward understanding the structural basis for the function of the calmodulin superfamily, we are carrying out solution structure determinations for calcium-free and calcium-bound calbindin D_{9k}. The small size (M_r 8500), high solubility, and stability of this protein make it very suitable for study by high-resolution ^1H NMR. Native calbindin D_{9k} and a variety of mutants produced by recombinant DNA techniques have been the focus of a series of biophysical studies (Brodin et al., 1986; Linse et al., 1987, 1988; Forsén et al., 1988; Wendt et al., 1988). During initial 2D NMR studies of the Ca^{2+}-saturated protein, an equilibrium between two forms in a 1:3 ratio was detected. Sequence-specific ^1H NMR assignments determined simultaneously for the two forms provided unambiguous evidence that the conformational heterogeneity was the result of cis–trans isomerism of Pro43 (Chazin et al., 1989a). This conformational heterogeneity is not specific to the recombinantly expressed bovine calbindin D_{9k}; proline isomerism is observed in solutions of native protein purified from bovine as well as porcine intestines. Proline cis–trans isomerism appears to play a central role in the folding and function of certain proteins [reviewed in Brandts and Lin (1986)], yet little is known about the structural consequences in proteins. Our ^1H NMR studies provide a unique opportunity to measure the rate of proline isomerization in the folded protein and to analyze the structural differences between the *cis*-Pro43 and *trans*-Pro43 isoforms of calbindin D_{9k}. The complete ^1H NMR assignments, secondary structure analyses, and global folding patterns of the major (*trans*-Pro43) form of bovine and porcine calbindin D_{9k} in the Ca^{2+}-bound state have been reported [Kördel et al. (1989) and Drakenberg et al. (1989), respectively]. Here, we present the corresponding analysis for the minor (*cis*-Pro43) form of the bovine protein, and compare the two isoforms.

The presence of two isoforms in solutions of calbindin D_{9k} presents serious problems for obtaining distance constraints from NOESY spectra for the determination of accurate three-dimensional solution structures. The principal difficulty is the inability to distinguish the relative contribution to cross-peak intensity, if corresponding cross peaks of the major and minor forms are degenerate. For example, it is conceivable that the distance between two protons could be significantly shorter in the minor form than that in the major form, yet corresponding chemical shifts are the same. Thus, a weak contribution from the major form cannot be distinguished from a strong contribution from the less abundant minor form. This problem has been circumvented by producing a mutant protein with Pro43 substituted by glycine (P43G). In this paper, the complete sequence-specific assignment of the ^1H NMR spectrum of the P43G mutant and a comparative analysis of this mutant with the wild-type protein is presented. On the basis of these results, we are able to assess differences in the structure and dynamics of the mutant, relative to native calbindin D_{9k}, and establish the suitability of replacing the wild-type protein with this mutant for determination of three-dimensional structures.

Materials and Methods

The methods for gene synthesis, modification, and expression are published (Brodin et al., 1986; Linse et al., 1987). Protein purification followed the modified procedure described in Chazin et al. (1989b).

Sample preparation and acquisition of 2D ^1H NMR spectra for the wild-type protein are as described in Kördel et al. (1989). The sample of P43G mutant was dissolved in 0.42 mL of ^1H_2O, containing 5% (v/v) ^2H_2O for the lock, to a concentration of 5 mM. The pH was adjusted to 6.0 by addition of microliter amounts of 0.01 M NaOH and HCl. To prepare the ^2H_2O sample, the same solution was lyophilized and then redissolved under argon in 0.42 mL of ^2H_2O. The pH* (no corrections for isotopic effects) was adjusted to 6.0 with 0.01 M NaO^2H and ^2HCl. The [^1H-(Ser, Val)-^2H]-calbindin (Brodin et al., 1989) used for the measurement of the rate of cis–trans isomerization was dissolved in 0.45 mL of ^2H_2O to a concentration of 1 mM. The pH* was adjusted to 6.0 with NaO^2H and ^2HCl as above.

The 1D ^1H NMR temperature study of the deuterated wild-type protein was made using a GE Ω 500 spectrometer. All ^1H NMR experiments on P43G were performed at 300 K using Bruker AM-500 spectrometers equipped with Aspect 3000 computers and digital phase-shifting hardware. COSY (Marion & Wüthrich, 1983) and DR-COSY (Wagner, 1983) spectra were recorded by utilizing standard-phase cycling and pulse sequences in the phase-sensitive mode. Pure absorption NOESY spectra were acquired by using the standard pulse sequence (Macura & Ernst, 1980) followed by a short Hahn-echo period to improve the quality of the base line [Dr. M. Rance, unpublished; Davis (1989)]. Time-proportional phase incrementation (Marion & Wüthrich, 1983) was used to achieve quadrature detection in the ω_1 dimension and the carrier was placed on the solvent resonance.

Three spectra were acquired from the ^1H_2O solution of P43G: COSY with 48 scans/t_1 value and a t_{1max} of 79 ms; DR-COSY (τ_1 = 22 ms, τ_2 = 40 ms) with 192 scans and t_{1max} = 51 ms: Hahn-echo NOESY (τ_m = 200 ms) with 160 scans and t_{1max} = 43 ms. In addition, a 2QF-COSY spectrum with 32 scans and t_{1max} = 94 ms and a Hahn-echo NOESY spectrum (τ_m = 200 ms) with 112 scans and t_{1max} = 61 ms were acquired from the ^2H_2O solution. The data were processed as described in Chazin et al. (1988) by use of an Aspect 3000 data station with Bruker software or a SUN 3/160C computer with the FTNMR software (kindly provided by Dr. D. Hare and modified for use on the SUN by Dr. J. Sayre). Vicinal backbone coupling constants ($^3J_{HN\alpha}$) were measured as described by Marion and Wüthrich (1983).

^{43}Ca and ^{113}Cd NMR experiments were performed as described in detail in Linse et al. (1987), except that the pH* of the ^{43}Ca NMR sample was adjusted to 7.5 instead of 8.0. The Quin2 method was used to determine the Ca^{2+}-binding constants (Linse et al., 1987). The latter measurements were repeated three times and the averaged result is reported.

Results and Discussion

The results reported here follow closely upon the detailed analysis of the major (*trans*-Pro43) isoform of calbindin D_{9k}. We specifically note that supporting documentation presented in Chazin et al. (1989a) and Kördel et al. (1989) is integral to the interpretation of some of the data presented below.

Determination of the Rate of Proline Cis–Trans Isomerization. The rate of proline isomerization in the Ca^{2+}-loaded form of calbindin D_{9k} is sufficiently slow at room temperature to result in well-resolved signals from the cis and trans isoforms. The rate can be measured by observation of the coalescence of corresponding resonances from the two isoforms in the 1D ^1H NMR spectrum as a function of temperature. Fortunately, calbindin D_{9k} is a very heat stable protein; the Ca^{2+}-saturated form of the protein cannot be heat denatured below 100 °C (Wendt et al., 1988) and the ^1H NMR spectrum is identical before and after the high-temperature NMR experiments. These observations provide important evidence that during the high-temperature studies the protein remains intact and that the coalescence phenomenon is not the result of irreversible denaturation.

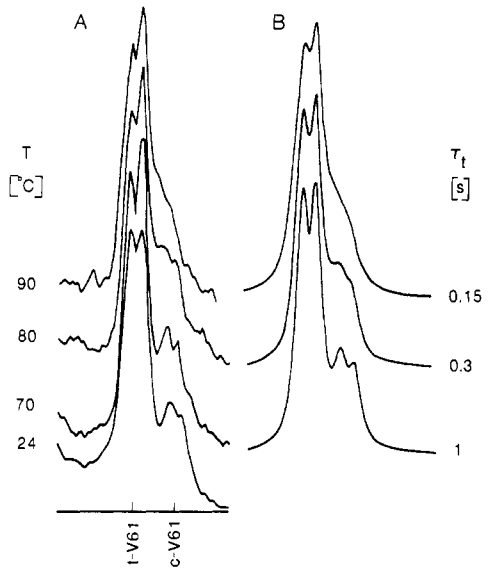

FIGURE 1: Determination of the Pro43 cis–trans exchange rate in calbindin D_{9k}. Depicted at different temperatures in (A) are the 500-MHz 1D signals of one of the Val61 C^{γ} methyl groups from the *trans*-Pro43 (*t*-V61) and *cis*-Pro43 (*c*-V61) isoforms of a special preparation of r-calbindin in which all amino acids except serines and valines are deuterated (Brodin et al., 1989). In (B) band shapes fitted to the experimental data are shown. These band shapes were calculated by use of a simple model of two exchanging AX spin systems taking the *J* coupling into account (McConnell, 1958). The theoretical band shapes are labeled with the corresponding calculated lifetimes for the trans form.

The drawback with 1D NMR spectroscopy is the poor peak resolution for larger molecules. To circumvent this problem, a special preparation of r-calbindin in which all amino acids except valine (and serine[3]) are deuterated was used (Brodin et al., 1989). In this sample, the minor and major Val61 $C^{\gamma}H_3$ doublets are fully resolved from all other peaks, thus permitting study of their temperature dependence in 1D spectra. Figure 1 shows that the major and minor forms of the protein are in chemical exchange and reach coalescence near 90 °C. The temperature dependence and line shape of these two doublets have been fitted by a standard model of two exchanging AX spin systems (McConnell, 1958). T_2 and the population ratio were adjusted by using a trans-form lifetime (τ) of 100 s to reproduce the experimental line shape at room temperature (24 °C). The best fit was obtained with the equilibrium population of the major (trans) isoform set to 75% and T_2 to 0.06 s for both resonances. A spin–spin coupling of 7.5 Hz was used, and to fully characterize the wild-type calbindin D_{9k}, calculated line shapes were matched with the experimental results by varying the lifetime of the trans form. The lifetimes for the trans form determined at 70, 80, and 90 °C were ~1, 0.3, and 0.15 s, respectively. Estimation of the trans lifetime at 25 °C by extrapolation from the measurements at 80 and 90 °C (the data point at 70 °C is not sufficiently accurate) gives a value of 15 s. This corresponds to a cis → trans exchange rate of 0.2 s^{-1}, from which a free energy of activation ($\Delta G^{\ddagger}$) of 77 kJ/mol is calculated.

Proline cis → trans interconversion rates have been measured for a large number of model peptides by Grathwohl and Wüthrich (1981). For example, exchange rates of 0.0022 and 0.03 s^{-1} are found at 25 °C for H-Gly-Pro-OH and H-Gly-Gly-Pro-Ala-OH, respectively. Interestingly, steric restriction by chain elongation and/or cyclization consistently increased the rate for proline cis–trans interconversion. On the basis of these latter observations, Grathwohl and Wüthrich proposed that appreciably faster rates might be found for globular proteins. Alternatively, the constraints imposed by the protein fold could reduce the rate of cis–trans isomerization in a globular protein relative to that in a small peptide. The fast rate in calbindin D_{9k} is consistent with the first hypothesis, apparently demonstrating that specific orientational effects in the folded protein can facilitate proline isomerization relative to a peptide (which samples a much wider range of conformational space). We hope to gain further insight into this issue from our detailed analysis of the three-dimensional solution structure and internal dynamics of r-calbindin.

Sequence-Specific Assignments of cis-Pro43 Calbindin D_{9k}. The fundamental step in any detailed ^1H NMR study is the assignment of resonances to specific hydrogen atoms in the molecule (sequence-specific assignments). To accomplish this, first the ^1H spin systems of each amino acid residue are identified according to amino acid type via scalar (through-bond) coupling, then each spin system is assigned to the appropriate location in the sequence based on the characteristic NOEs (through-space couplings) between backbone amide, C^{α}, and C^{β} protons of residues adjacent in the sequence (Billeter et al., 1982).

The identification of spin systems starts with examination of the backbone fingerprint region of a COSY spectrum recorded in ^1H_2O. For bovine calbindin D_{9k}, this region should contain cross peaks for 71 residues (76 amino acids, minus 4 prolines and the rapidly exchanging primary amine of MetO). However, it was apparent upon initial inspection of the spectrum that this (and all other) region(s) contained far more than the expected number of cross peaks. Thorough analysis by analytical biochemical techniques and 2D ^1H NMR suggested that all cross peaks arise from two isoforms of a single chemical species. This hypothesis was confirmed by observation of chemical-exchange cross peaks [see Figure 2 of Chazin et al. (1989a)].

The presence of two species in solution meant that it was necessary to take great care in attributing cross peaks in the 2D spectra. Since cross-peak intensity has a strong dependence on either the magnitude of the active spin coupling or the dipolar coupling (distance to the nearest proton), it cannot be used as a reliable indicator of relative concentration. This is particularly evident in the backbone fingerprint region of COSY spectra, where some cross peaks from the minor form are stronger than their counterparts in the major form, even though the trans isoform is more abundant by a factor of 3. This complicating factor made it essential to obtain the complete sequence-specific assignments for both forms in parallel, separately characterizing each form as completely as possible. In order to achieve this, it was imperative to acquire the 2D spectra with high digital resolution and sufficient sensitivity to detect all of the weak cross peaks arising from the minor isoform and then to identify all resolved cross peaks. Separate pathways of sequential connectivities can be identified, which provides an unambiguous means for differentiating major and minor spin systems and for assigning them to the *trans*-Pro43 and *cis*-Pro43 isoforms, respectively (Chazin et al., 1989a).

The ^1H spin systems of the major (*trans*-Pro43) isoform of bovine calbindin D_{9k} have been identified (Kördel et al., 1989) by using the general assignment strategy described in Chazin et al. (1988). To assign the resonances of the minor (*cis*-Pro43) isoform, we have taken advantage of the fact that most of the chemical shifts of the two isoforms are very similar. A

[3] The incorporation of [^1H]Ser in this preparation played no role in these measurements, but enhanced the utility of the sample for use in other experiments.

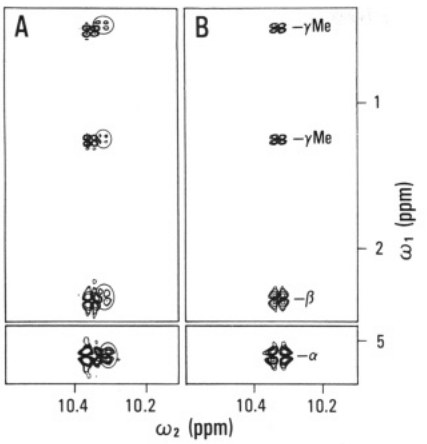

FIGURE 2: Comparison of side-chain proton connectivities observed at the backbone amide proton resonance of Val61 in wild-type (A) and P43G (B) r-calbindin. The DR COSY spectra were acquired at 500 MHz on 4–5 mM samples in unbuffered solution at pH 6.0 and 300 K. See text for further details.

typical example is shown in Figure 2A, where the direct and relayed cross peaks to the amide proton resonance of Val61 in the minor form appear as shadows to the high-field side of the corresponding connectivities in the major form. This degree of similarity permitted assignment of a large number of resonances of the minor isoform by direct comparison with the major isoform. These tentative assignments were verified by checking for the expected sequential NOE connectivities. This left only a subset of residues, Ser38–Leu53, for which assignments had to be made ab initio, identifying spin systems and applying the sequence resonance assignment procedure. For this polypeptide segment, a series of $d_{NN}(i, i + 1)$ connectivities link the sequence from Ser38 to Gly42. Between Gly42 and Pro43, one observes the characteristic $d_{\alpha\alpha}(i, i + 1)$ NOE for a X-Pro cis peptide bond in the minor form, [and the typical $d_{\alpha\delta}(i, i + 1)$ NOE for a X-Pro trans peptide bond in the major form]. Both $d_{\alpha N}$ and $d_{\delta N}$ connectivities are observed between Pro43 and Ser44. At pH 6.0 and 300 K, the $d_{\alpha N}$ between Ser44 and Thr45 cannot be observed due to saturation of the $C^{\alpha}H$ resonance of Ser44 from the suppression of the water signal; however, a strong $d_{\beta N}$ connectivity is present. A $d_{\alpha N}$ NOE from Thr45 to Leu46 followed by successive d_{NN} connectivities from Leu46 to Asp54 (all resolved from the major form) completes the sequential assignment of the Ser38–Asp54 spin systems of the minor form. The assignments for the minor isoform that have at least one chemical shift significantly different from that in the major isoform [Table I of Kördel et al. (1989)] are identified in Figure 3 (backbone protons) and Table I (side-chain protons).

Comparison of cis-Pro43 and trans-Pro43 Calbindin D_{9k}. In this section, the structural consequences of cis–trans isomerization of Pro43 are examined by comparing chemical shifts, backbone scalar coupling constants, and sequential NOEs of the two isoforms. Although chemical shifts in themselves yield very limited information about protein conformation, they are very sensitive probes of structural differences between proteins [e.g., Pardi et al (1983)]. From inspection of the chemical shift differences ($\Delta\delta$s) in Figure 3 and chemical shifts in Table I, it appears that the conformational changes upon cis–trans interconversion are localized to the region in close spatial proximity to Pro43 while the global structure remains intact. Differences in chemical shift are found mostly in the linker loop between the two calcium-binding domains (Phe36–[Pro43]–Ser44), and in the immediately adjacent helix III of domain II (Thr45–Asp54). The largest differences in chemical

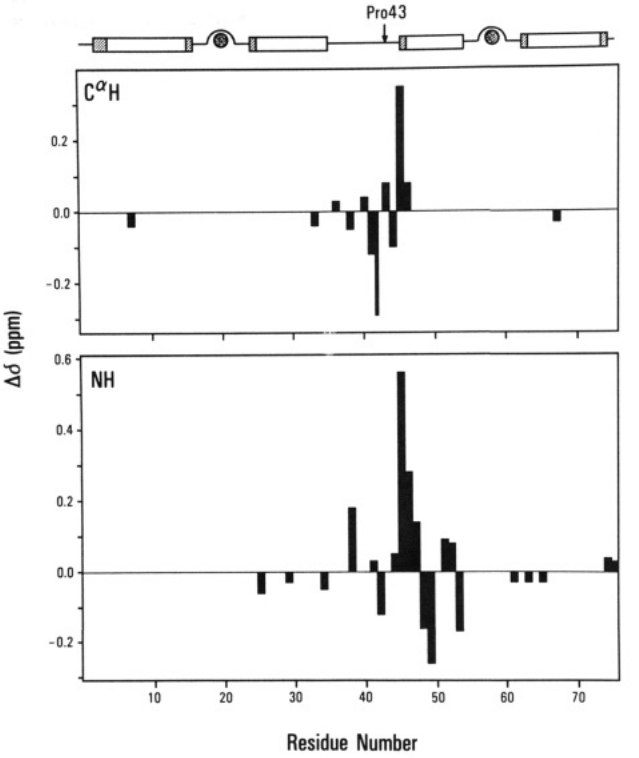

FIGURE 3: Backbone chemical shift differences ($\Delta\delta > 0.02$ ppm) versus residue number for the two isoforms of wild-type calbindin D_{9k}, at pH 6.0 and 300 K. Positive values represent downfield shifts and negative values upfield shifts for the minor *cis*-Pro43 isoform, relative to the major *trans*-Pro43 isoform. The experimental uncertainty in these numbers is ±0.01 ppm. The sequence location of structural elements is indicated schematically above. Helices are identified by cylinders with crosshatching for frayed or irregular segments. The two large circles represent calcium ions and the loops above them identify the approximate locations of the calcium-binding loops.

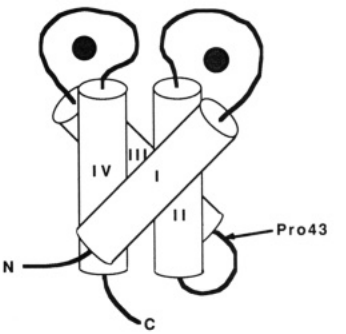

FIGURE 4: Schematic diagram of calbindin D_{9k}. Helices are indicated by cylinders and the Ca^{2+} ions as shaded spheres.

shift along the backbone are observed for the Gly42 and Thr45 spin systems. Interestingly, it is the $C^{\beta}H/C^{\gamma}H_3$ cross peak of Thr45, two residues distant from the site of isomerization, that exhibits the largest difference in side-chain chemical shift. In the following, we provide a rationale for the observed effects on chemical shifts for those protons that are not immediately adjacent to Pro43, by reference to the information available about the structure of the major (*trans*-Pro43) isoform of r-calbindin in solution (Kördel et al., 1989) and in crystals (Szebenyi & Moffat, 1986). A schematic diagram of the three-dimensional structure of the protein is shown in Figure 4.

A majority of the residues in helix III (Thr45–Asp54) show at least one backbone or side-chain proton with $\Delta\delta > 0.02$ ppm (Figure 3). These widespread differences are the result of either perturbation of the helix itself or a change in the in-

Table I: ^{1}H NMR Chemical Shifts of the Side Chains of the Minor (*cis*-Pro43) Isoform of Bovine Calbindin D_{9k} That Differ from the Major (*trans*-Pro43) Isoform at pH 6.0 and 300 K[a]

residue	chemical shifts (ppm)			
	C^β	C^γ	C^δ	other
Y13	2.43, 2.82			7.42, 6.74 ($C^\delta H$, $C^\epsilon H$)
T34	4.14	1.24		
F36	2.75, 3.32			7.14, 7.01, 7.12 ($C^\delta H$, $C^\epsilon H$, $C^\zeta H$)
P37	2.42, 1.21	1.96, (1.96)[b]	3.09, 3.53	
S38	3.92, 3.98			
L40	1.66, 1.85	1.55	0.81, 0.94	
K41	1.90, 1.99	1.41, 1.48	1.64, 1.70	2.99, 2.99 ($C^\epsilon H_2$)
P43	2.18, 2.32	1.85, 1.94	3.50, 3.67	
S44	3.75, 3.91			
T45	4.70	1.32		
D47	2.49, 2.69			
L49	1.60, 1.75	1.64	0.79, 0.83	
F50	2.96, 3.22			7.11, 7.12, 7.15 ($C^\delta H$, $C^\epsilon H$, $C^\zeta H$)
E51	2.08, 2.11	2.35, 2.46		
L53	1.11, 1.66	2.03	0.74, 0.82	
D54	1.61, 2.53			
V61	2.33	0.46, 1.24		
F63	2.44, 2.66			6.49, 7.13, 7.35 ($C^\delta H$, $C^\epsilon H$, $C^\zeta H$)
V68	1.95	0.84, 1.02		
L69	1.21, 1.31	1.25	0.57, 0.70	
I73	1.74	0.71, 1.20	0.19	0.60 ($C^\gamma H_3$)
Q75	1.96, 2.12	2.32, (2.32)[b]		6.80, 7.50 ($N^\epsilon H_2$)

[a] Chemical shifts are referenced to the H_2O signal at 4.75 ppm and are generally accurate to ±0.02 ppm (±0.03 ppm for geminal protons separated by <0.1 ppm). Chemical shifts that are not identical in the two isoforms are underlined, and those for which $\Delta\delta > 0.05$ ppm are doubly underlined. [b] Degeneracy is assumed.

terface between the helix and the rest of the protein. The differences in chemical shifts for Val61 in Ca^{2+}-binding loop II are attributed to close contact with the perturbed helix III, as evidenced by NOEs between both Leu53 $C^\delta H_3$ groups and one of the Val61 $C^\gamma H_3$ groups. The differences observed in the chemical shifts of protons in Ca^{2+}-binding loop I are most likely caused by transmission of the changes in loop II through the hydrogen bonds between Leu23 and Val61. The NOE connectivity between the C^ϵ protons of Lys25 and the two degenerate C^δ methyl groups of Leu46 indicates that helix III is also in contact with helix II and provides a rationale for changes in the chemical shifts of Lys25.

In helix IV (Ser62–Ser74), $\Delta\delta > 0.02$ ppm is observed for the backbone as well as the side-chain protons of the C-terminal residues Ile73–Gln75, apparently the result of contacts between Ile73 and the N-terminal portion of the linker loop. Since NOEs are observed between Ile73 and both the Phe36 and the Phe66 aromatic rings, the differences in chemical shift for residues at the C-terminus may be associated with subtle changes in the packing of the hydrophobic core of the protein. A similar explanation is possible for the only other chemical shift differences observed in helix IV, involving the side chain of Leu69, since this residue has close contacts with the aromatic ring of Phe66 (Leu69 $C^\delta H_3$/Phe66 $C^\delta H$ NOE). In helix I (Ser2–Lys16), only the $C^\alpha H$ shift of Lys7 and the shifts of the C^β and C^δ protons of the Tyr13 side chain are distinctively perturbed. Since the aromatic ring of Phe63 is in contact with the backbone protons of Lys7 (NOE between Lys7 NH and Phe63 $C^\epsilon H$), small changes in the packing of the hydrophic core could explain the difference in the chemical shift of the $C^\alpha H$ of Lys7. NOEs from Tyr13 $C^\delta H$ to one of the Leu30 C^δ methyl groups and the Gln33 C^β protons, and observation of a hydrogen bond between the hydroxyl proton of Tyr13 and the carboxylate of Glu35 (Szebenyi & Moffat, 1986), indicate that the tyrosine ring is in contact with the C-terminal half of helix II (Ser24–Glu35) and the N-terminus of the linker loop. This provides a rationale for chemical shift differences of protons of Tyr 13.

Backbone scalar coupling constants ($^3J_{HN\alpha}$) could be measured for only 15 residues of the minor isoform, due to cross-peak degeneracy. Significant differences (>1 Hz) in $^3J_{HN\alpha}$ were observed for Lys25, Ser38, Thr45, Leu49, and Asp54; however, none of these differences are greater than 2 Hz. The differences in the conformation of the peptide backbone of the two isoforms are therefore very small.

At the Gly42–Pro43 peptide bond, $d_{\alpha\delta}(i, i+1)$ connectivities are observed for the major isoform, whereas $d_{\alpha\alpha}(i, i+1)$ connectivities are observed for the minor isoform. These NOEs identify the presence of trans and cis peptide bonds, respectively (Billeter et al., 1982). A detailed comparison of sequential NOEs shows no other distinctive differences for corresponding residues of the two isoforms; thus, there are no other substantial structural differences in the peptide backbone of the two isoforms.

Characterization of Ion-Binding Properties of P43G. ^{113}Cd and ^{43}Ca NMR have been used as probes of the calcium-binding loops, monitoring structural changes during titration with calcium or cadmium [reviewed in Vogel & Forsén (1987)]. Macroscopic calcium-binding constants have been determined by titrating the protein with Ca^{2+} in presence of a fluorescent Ca^{2+} chelator (Quin2). Ca^{2+}-exchange rates have been measured by using ^{43}Ca NMR line widths (Drakenberg et al., 1983; Tsai et al., 1987). Characterization of Ca^{2+} and Cd^{2+} binding for the wild type have been reported (Linse et al., 1987). The results for P43G are very similar to those for the wild-type protein (Table II). However, whereas the free energies of Ca^{2+} binding are identical within experimental error, the dissociation rate constant (k_{off}) for the Ca^{2+} ions bound to P43G is approximately 6 times higher than for the wild-type protein. We do not, as yet, have an explanation for

Table II: Characterization of Binding Properties of Pro43 → Gly and Wild-Type r-Calbindin[a]

		^{43}Ca NMR		^{113}Cd NMR		calcium binding		
protein	site	k_{off} (s^{-1})	δ (ppm)	δCd1 (ppm)	δCd2 (ppm)	K_1 (10^8 M^{-1})	K_2 (10^8 M^{-1})	ΔG (kJ/mol)
wild type	I	≤10	−9		~−150	1.6 ± 0.4	4.0 ± 0.4	−96
	II	≤10	7	−105	−110			
Pro43 → Gly	I	60	−9		~−150	0.9 ± 0.4	5.0 ± 0.4	−95
	II	60	7	−105	−110			

[a] Experimental values have been reported (Linse et al., 1987) for samples that later have been found to contain deamidation products (Chazin et al., 1989b). Unpublished experiments by C. Johansson confirm that the results from ^{43}Ca and ^{113}Cd NMR are identical for intact and deamidated wild-type r-calbindin. Ca^{2+}-binding constants do, however, differ slightly. Redetermined values for intact wild-type r-calbindin are therefore reported here (S. Linse, unpublished experiments).

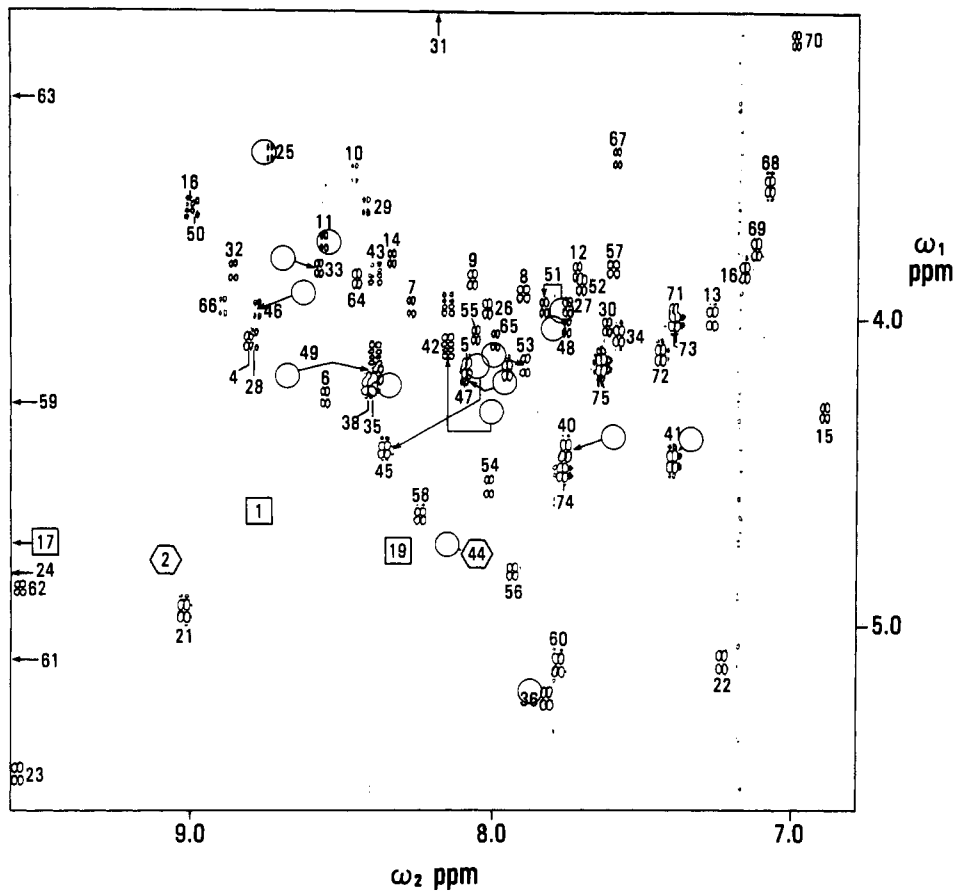

FIGURE 5: Backbone fingerprint region of a 500-MHz COSY spectrum of 5 mM P43G r-calbindin at 300 K and pH 6.0. The ω_1 = C$^\alpha$H, ω_2 = NH cross peaks are labeled with the sequence-specific assignments. Circles indicate the position of the corresponding cross peaks of native r-calbindin that differ by more than 0.03 ppm in either C$^\alpha$H or NH chemical shift. The few cross peaks that appear outside the region shown are indicated with arrows. Boxes show the location of cross peaks not observed in this spectrum, but which could be identified in other 2D spectra. Hexagons are drawn around cross peaks that can only be observed at very low contour levels.

this slightly larger k_{off} rate for P43G, although it is important to note that it is 1–2 orders of magnitude lower than the effects induced by mutation in one of the calcium-binding sites; the k_{off} values for mutants P20G, P20G + N21Δ, and P20Δ are 43, 500, and 500 times larger than that for the wild-type protein (Linse et al., 1987).

Sequence-Specific Assignments of Pro43 → Gly Calbindin D_{9k}. From a quick comparison of the COSY backbone fingerprint regions of the wild-type and P43G proteins, it is clear that the chemical shift differences (and by inference, structural differences) are small enough to make assignments by comparison. We have therefore followed the protocol used for obtaining sequence-specific assignments of the minor isoform of wild-type r-calbindin. Initially, the NH/C$^\alpha$H cross peaks in the COSY spectrum of P43G were tentatively assigned to the closest cross peak in the corresponding spectrum of the wild-type protein. The backbone fingerprint of P43G is shown in Figure 5, along with the position of the corresponding cross peaks that differ by more than 0.03 ppm (circles) in the major (*trans*-Pro43) isomer of the wild-type protein. While 71 C$^\alpha$H/NH cross peaks are expected, only 68 are found. The three missing peaks are bleached out by the irradiation of the water signal. The chemical shifts of the protons of the side-chain methyl groups, the aromatic rings, the side-chain amides, and the single observable hydroxyl proton (of Ser62) could also be identified in the COSY spectrum. The DR-COSY spectrum yielded 109 out of the 130 C$^\beta$ proton resonances and 10 C$^\gamma$ proton resonances, bringing the total number of assigned resonances to approximately 70%.

The sequential resonance assignments were then traced in the NOESY spectrum, as documented previously for *trans*-Pro43 calbindin D_{9k} (Kördel et al., 1989). The crucial NOEs necessary to establish the sequential assignments for the Ser38–Leu53 segment are shown in Figure 6. Strong $d_{NN}(i, i + 1)$ connectivities are observed for the polypeptide segment Ser38–Lys41. A strong $d_{\alpha N}(i, i + i)$ and a weak $d_{NN}(i, i + 1)$ bridge the sequence to Gly42, followed by $d_{\alpha N}(i, i + 1)$ connectivities from Gly42 to Gly43 and from Gly43 to Ser44.

Table III: ^{1}H NMR Chemical Shifts of P43G Calbindin D_{9k} (pH 6.0, 300 K)[a]

residue	chemical shifts (ppm)					
	NH	C^α	C^β	C^γ	C^δ	other
M0		[4.27	1.88, 1.96	2.19, (2.19)[b]][c]		2.09 ($C^\epsilon H_3$)
K1	(8.76)[c]	4.60	1.78, 1.80	1.62, (1.62)[b]	1.73, 1.73	2.95, 2.95 ($C^\epsilon H_2$)
S2	9.07	4.78	4.06, 4.44			
P3		4.32	2.00, 2.48	2.05, 2.23	3.98, 3.98	
E4	8.80	4.08	1.98, 2.09	2.27, 2.46		
E5	8.08	4.16	2.07, 2.43	2.25, 2.44		
L6	8.54	4.26	1.70, 2.19	1.88	0.95, 1.03	
K7	8.26	3.97	1.78, 1.90	0.80, 1.16	1.36, 1.36	2.61, 2.67 ($C^\epsilon H_2$)
G8	7.89	3.92, 3.92				
I9	8.06	3.87	2.21	1.20, 1.99	0.98	1.17 ($C^\gamma H_3$)
F10	8.45	3.53	2.67, 3.31			6.32, 7.11, 7.62 ($C^\delta H$, $C^\epsilon H$, $C^\zeta H$)
E11	8.56	3.75	1.95, 2.10	2.32, 2.68		
K12	7.72	3.85	1.74, 1.79	0.54, 1.08	1.42, 1.50	2.71, 2.71 ($C^\epsilon H_2$)
Y13	7.27	4.00	2.44, 2.80			7.44, 6.75 ($C^\delta H$, $C^\epsilon H$)
A14	8.33	3.80	0.43			
A15	6.89	4.30	1.43			
K16	7.16	3.85	1.97, 2.14	1.48, 1.56	1.64, 1.72	2.74, 2.95 ($C^\epsilon H_2$)
E17	9.71	4.72	1.89, 2.00	1.95, 2.22		
G18	9.00	3.64, 3.95				
D19	8.33	4.69	2.63, 2.86			
P20		4.80	2.01, 2.22	1.89, 2.07	4.01, 4.01	
N21	9.01	4.95	2.69, 3.00			7.94, 6.96 ($N^\delta H_2$)
Q22	7.23	5.12	1.83, 2.12	2.02, 2.25		6.56, 7.48 ($N^\epsilon H_2$)
L23	9.56	5.49	1.60, 2.02	1.31	0.38, 0.72	
S24	10.08	4.84	4.18, 4.37			
K25	8.73	3.46	0.44, 1.30	0.65, 1.05	1.39, 1.40	2.53, 2.58 ($C^\epsilon H_2$)
E26	8.01	3.97	1.88, 1.96	2.22, 2.32		
E27	7.75	3.97	1.86, 2.36	(2.27, 2.45)[c]		
L28	8.78	4.07	1.56, 2.32	1.73	1.06, 1.12	
K29	8.42	3.64	1.91, 2.10	1.20, 1.33	1.63, (1.63)[b]	2.81, 2.86 ($C^\epsilon H_2$)
L30	7.62	4.03	1.75, 1.86	1.87	0.99, 0.99	
L31	8.15	2.34	1.19, 1.74	1.23	0.79, 0.93	
L32	8.85	3.85	1.35, 1.95	2.02	0.79, 0.92	
Q33	8.57	3.84	1.96, 2.17	2.37, 2.53		7.33, 6.77 ($N^\epsilon H_2$)
T34	7.58	4.06	4.16	1.22		
E35	8.40	4.21	1.28, 1.44	2.18, 2.67		
F36	7.81	5.24	2.75, 3.34			7.14, 7.01, 7.12 ($C^\delta H$, $C^\epsilon H$, $C^\zeta H$)
P37		4.18	2.43, (1.21)[c]	1.96, (1.96)[b]	3.08, 3.53	
S38	8.41	4.22	3.91, 3.98			
L39	7.95	4.17	1.59, 1.85	1.69	0.75, 0.75	
L40	7.75	4.43	1.69, 1.72	1.54	0.79, 0.93	
K41	7.40	4.46	1.73, 1.97	1.38, 1.46	1.64, 1.70	3.00, 3.00 ($C^\epsilon H_2$)
G42	8.14	3.95, 4.10				
G43	8.37	3.85, 4.12				
S44	8.03	4.76	3.78, 3.88			
T45	8.35	4.43	4.54	1.29		
L46	8.77	3.98	1.62, 1.84	1.55	0.94, 0.94	
D47	8.09	4.19	2.54, 2.70			
E48	7.75	4.03	2.00, 2.19	2.31, 2.37		
L49	8.37	4.18	1.58, 1.76	1.59	0.80, 0.84	
F50	8.98	3.64	2.98, 3.21			7.13, 7.12, 7.15 ($C^\delta H$, $C^\epsilon H$, $C^\zeta H$)
E51	7.83	3.97	1.88, 2.10	2.15, 2.34		
E52	7.70	3.89	2.07, 2.12	2.00, 2.25		
L53	7.89	4.15	1.12, 1.64	2.02	0.73, 0.82	
D54	8.01	4.55	1.58, 2.51			
K55	8.05	4.05	1.87, (1.94)[c]	1.50, 1.60	1.74, 1.74	3.09, 3.13 ($C^\epsilon H_2$)
N56	7.93	4.82	2.85, 3.30			6.63, 8.03 ($N^\delta H_2$)
G57	7.60	3.84, 3.84				
D58	8.23	4.64	2.45, 3.14			
G59	10.50	3.71, 4.27				
E60	7.77	5.13	1.44, 1.90	2.01, 2.17		
V61	10.33	5.10	2.35	0.48, 1.25		
S62	9.55	4.88	4.20, 4.51			5.98 ($O^\gamma H$)
F63	9.60	3.28	2.45, 2.65			6.49, 7.13, 7.35 ($C^\delta H$, $C^\epsilon H$, $C^\zeta H$)
E64	8.45	3.87	1.89, 2.05	2.24, (2.24)[b]		
E65	7.99	4.07	1.65, (1.84)[c]	2.35, 2.57		
F66	8.89	3.96	3.11, 3.27			6.91, 7.16, 7.09 ($C^\delta H$, $C^\epsilon H$, $C^\zeta H$)
Q67	7.58	3.48	1.89, 1.94	2.15, 2.34		5.74, 6.15 ($N^\epsilon H_2$)
V68	7.08	3.57	1.95	0.83, 1.03		
L69	7.12	3.78	1.19, 1.30	1.27	0.57, 0.71	
V70	6.99	3.10	1.96	0.62, 0.76		
K71	7.40	3.97	1.74, 1.82	(1.40),[c] 1.46	1.60, 1.60	2.90, 2.90 ($C^\epsilon H_2$)
K72	7.44	4.12	1.83, 1.86	1.48, (1.54)[c]	1.45, 1.60	2.72, 2.84 ($C^\epsilon H_2$)
I73	7.39	4.01	1.74	0.70, 1.19	0.18	0.59 ($C^\gamma H_3$)

Table III (Continued)

residue	chemical shifts (ppm) NH	C^{α}	C^{β}	C^{γ}	C^{δ}	other
S74	7.76	4.50	3.86, 3.86			
Q75	7.64	4.15	1.94, 2.10	2.30, (2.30)[b]		6.78, 7.50 ($N^{\epsilon}H_2$)

[a] Chemical shifts are referenced to the H_2O signal at 4.75 ppm and are generally accurate to ±0.01 ppm (±0.03 ppm for germinal protons separated by <0.1 ppm). Chemical shifts in P43G that differ by more than 0.05 ppm with respect to the major (*trans*-Pro43) isoform of the wild-type protein are underlined. Those that differ by more than 0.10 ppm are doubly underlined. [b] Degeneracy assumed. [c] No experimental evidence found in the limited subset of spectra acquired for P43G, but the assignment is assumed to be the same as for the major (*trans*-Pro43) isoform of wild-type r-calbindin because all other ^1H resonances of the side chain were found to be identical within experimental error. The uncertainty for these values is ±0.04 ppm. Due to severe spectral crowding, only the C^{ϵ} methyl of Met0 has been specifically identified.

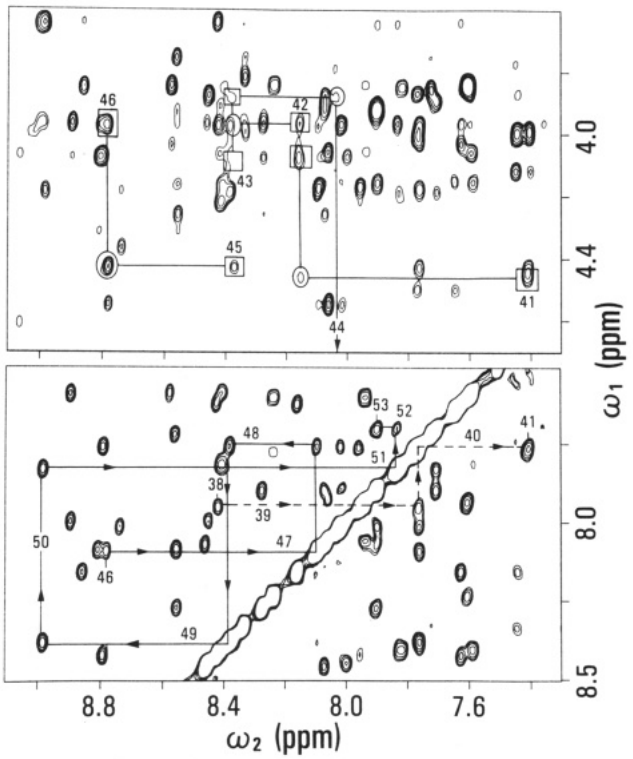

FIGURE 6: Sequential resonance assignments for the polypeptide segment Ser38–Leu53. Region of a 500-MHz Hahn-echo NOESY spectrum (τ_m = 200 ms) of a 5 mM ^1H_2O solution of P43G r-calbindin at 300 K and pH 6.0 showing sequential $d_{\alpha N}$ connectivities (upper panel) for the residues in extended conformation and d_{NN} connectivities (lower panel) for the helical segments. (Upper panel) NOE tracings of Gly42–Thr45. Cross peaks corresponding to $d_{\alpha N}(i, i + 1)$ NOE connectivities are boxed. Circles indicate the position of the COSY cross peaks found under identical conditions. A vertical line is drawn between the COSY cross peak and the sequential NOE cross peak for each amide proton and a horizontal line connects the NOE and COSY cross peaks for each C^{α} proton. (Lower panel) NOE tracings from Ser38 to Lys41 and from Leu46 to Leu53. Lines are drawn between pairs of $d_{NN}(i, i - 1)$ and $d_{NN}(i, i + 1)$ cross peaks (boxed) and are labeled with the sequence-specific assignments.

It is not possible to observe the Ser44 $C^{\alpha}H$/NH COSY cross peak at pH 6.0, 300 K, due to the irradiation of the water signal, but the $d_{\alpha N}(i, i + 1)$ connectivity between Ser44 and Thr45 is clearly present. A $d_{\alpha N}$ connectivity from Thr45 to Leu46 is followed by consecutive $d_{NN}(i, i + 1)$ connectivities for the polypeptide segment Leu46–Leu53. A summary of the sequential NOE connectivities for residues Lys29–Val61 is given in Figure 7, which also includes a comparison to those observed for the major isoform of the wild-type protein [cf., Figure 4 of Kördel et al. (1989)].

Once the backbone amide resonances were sequentially assigned, the remainder of each spin system was identified in the COSY, 2QF-COSY, and NOESY spectra, using the assignments from the major isoform of the wild-type protein as a guide. An essentially direct transfer of the side-chain assignments, even in the polypeptide segment Glu33–Leu53, is possible due to the high degree of similarity between the mutant and wild-type protein (Figure 2B). The complete set of assignments is given in Table III.

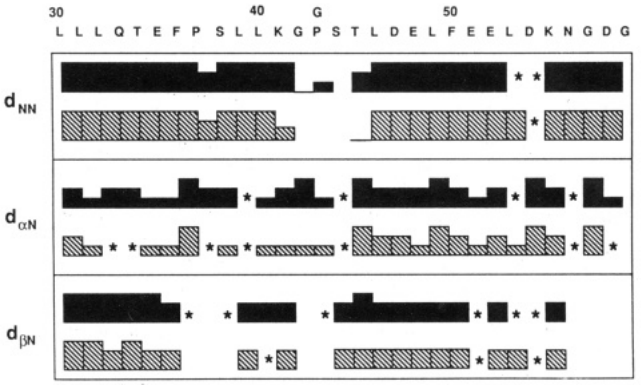

FIGURE 7: Comparison of the characteristic sequential NOE connectivities, $d_{NN}(i, i + 1)$, $d_{\alpha N}(i, i + 1)$, and $d_{\beta N}(i, i + 1)$, observed at 300 K, pH 6.0, in *trans*-Pro43 r-calbindin (filled bars) and P43G r-calbindin (hatched bars). The sequence is given at the top using the one-letter amino acid code. The height of the bars gives a qualitative measure of the relative strength of the NOE in the 200-ms NOESY spectrum. Connectivities to proline $C^{\delta}H_2$ resonances are listed in the location for the corresponding backbone amide proton. Connectivities that could not be identified at this temperature and pH due to degeneracy of resonances or as a byproduct of solvent saturation are labeled with an asterisk (*).

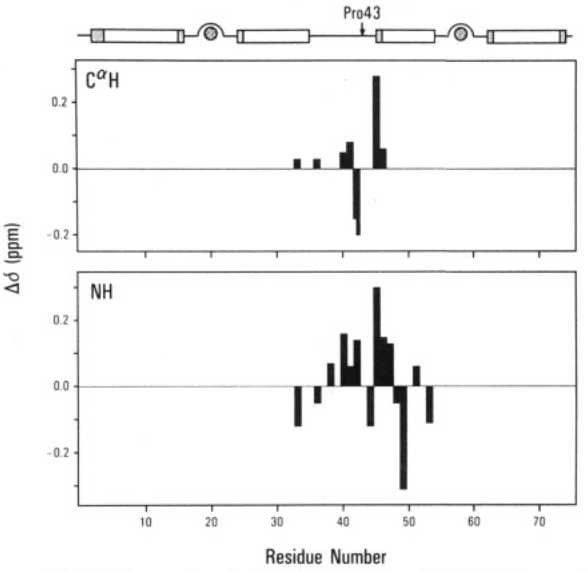

FIGURE 8: Backbone chemical shift differences ($\Delta\delta$ > 0.04 ppm for NH, $\Delta\delta$ > 0.02 ppm for $C^{\alpha}H$) plotted versus residue number for the major (*trans*-Pro43) isoform of calbindin D_{9k} and the P43G mutant, at pH 6.0 and 300 K. Positive values represent downfield shifts and negative values upfield shifts of the mutant, relative to the wild-type protein. The experimental uncertainty in these numbers is ±0.02 ppm. The sequence location of structural elements is indicated schematically above. See the caption to Figure 2 for further details.

Comparison of Pro43 → Gly and Wild-Type r-Calbindin. The backbone chemical shift differences between *trans*-Pro43 and P43G r-calbindin are shown in Figure 8. The uncertainty in the $\Delta\delta$ values is ±0.02 ppm, since these chemical shift differences are determined in *two* different experiments. Overall, the values are smaller than the differences between the *trans*- and *cis*-Pro43 forms (cf. Figure 2). Outside the polypeptide segment Ser38–Leu53, only the backbone NH and $C^{\alpha}H$ resonances of residues 33 and 36 are significantly different in the two proteins. The differences in chemical shift within the segment Thr45–Leu53 are similar in size and sign to those between the major and minor isoforms of the wild-type protein. Interestingly, the backbone chemical shifts of residues Thr45–Leu53 are closer to the *cis*-Pro43 form of r-calbindin. However, for the backbone NH resonances of Gly42 and Ser44, and for the $C^{\alpha}H$ resonances of Gln33 and Lys41, the signs of the $\Delta\delta$s for P43G are the opposite of those of the minor (*cis*-Pro43) isoform. This effect may be due to the substitution for the conformationally restricted proline by a residue with a higher degree of conformational freedom along the backbone. This substitution could result in an increase in the flexibility of the linker loop and an average structure that differs from those of the wild-type isoforms. The similarities of the chemical shifts of helix III in P43G to those in *cis*-Pro43 r-calbindin suggest that helix III or the interface between this helix and the rest of the protein in P43G is perturbed (relative to the major isoform) in a manner similar to the minor isoform (see above).

Only 10 P43G side-chain proton shifts differ by 0.05 ppm or more from the corresponding shifts of *trans*-Pro43 r-calbindin, discounting of course, the mutated residue 43. All of these 10 protons belong to amino acid residues in the polypeptide segment Leu40–Leu49. The $C^{\beta}H$ and $C^{\gamma}H_3$ shifts of Thr45 are the only shifts differing by more than 0.1 ppm (doubly underlined in Table III, while the other eight shifts are singly underlined). The side-chain perturbations relative to *trans*-Pro43 are thus spatially confined to the same region but are smaller in magnitude for P43G than for *cis*-Pro43 r-calbindin.

A comparison of the sequential NOEs found for P43G and wild-type r-calbindin over the Lys29–Val61 segment is given in Figure 7. The intensity of NOEs in P43G can be compared quantitatively only if the corresponding cross peaks for the two forms of the wild-type protein are resolved. With this in mind, the only distinctive differences in the sequential NOE patterns of P43G and *trans*-Pro43 r-calbindin, excluding those involving the mutated residue, are the lower intensities of the Thr45–Leu46 d_{NN} and $d_{\beta N}$ connectivities in the mutant. In other words, structural perturbation, if any, is highly localized to the residues flanking the site of mutation. All key tertiary NOEs, such as those defining the β-sheet and permitting the definition of the global fold of wild-type r-calbindin (Kördel et al., 1989), are virtually identical in the P43G and wild-type proteins.[4]

The values for the backbone spin–spin coupling constants $^3J_{HN\alpha}$ in *trans*-Pro43 and P43G r-calbindin are plotted versus the amino acid sequence in Figure 9. Any differences in $^3J_{HN\alpha}$ values observed between the two proteins are within the experimental error of the measurements. These results indicate that there are no significant differences in the backbone conformation of the two proteins.

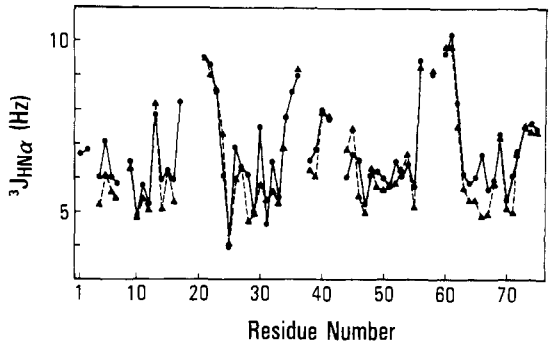

FIGURE 9: Comparison of backbone NH/$C^{\alpha}H$ spin–spin coupling constants ($^3J_{HN\alpha}$) of the major (*trans*-Pro43) isoform of calbindin D_{9k} (●) and the P43G mutant (▲). Data points for consecutive residues are connected with straight lines. The experimental uncertainty in these numbers is ±1Hz.

In summary, the ^1H NMR results for P43G show that the global structure of the Ca^{2+}-saturated state in solution is identical with the wild-type protein, and that there are significant, but highly localized structural perturbations near the site of mutation. The ^{43}Ca and ^{113}Cd results indicate that the kinetics of Ca^{2+} binding and the nature of the ligands coincide for the two proteins. Such minimal effects could be predicted on the basis of the location of Pro43 in the linker loop (Szebenyi & Moffat, 1986), and on the large number of reports of highly localized effects observed for a variety of amino acid substitutions [e.g., Markley et al. (1986), Pielak et al. (1988), Madison et al. (1989), Ringe (1989)] or chemical modifications [e.g., Wagner et al. (1979), Stassinopoulou et al. (1984), Chazin et al. (1985)] in other proteins.

Conclusions

The 2D ^1H NMR studies described in this work show that it is possible to completely assign the ^1H resonances of two different, but homologous, isoforms of a small protein, although the two forms are in equilibrium and unfavorably populated (3:1). The greatest difficulty involved in ^1H NMR studies of two inseparable and very similar molecules (or isoforms of the same molecule) is to account for cross peaks that are not resolved in the spectrum. The inability to locate a specific cross peak may be due to coincidence of the corresponding peaks of the two species or degeneracy with other cross peaks, or the cross peak may be simply not present. To complete the analysis of both the *trans*-Pro43 *and* the *cis*-Pro43 r-calbindin isoforms, we assigned every *resolved* peak observed in the 2D ^1H NMR spectra. In the light of the great similarity in the chemical shifts of most protons of the two isoforms, and of the assignment of all resolved peaks, we feel confident in assuming that for the residues not showing resolved peaks the resonances from the major and minor forms are degenerate.

Cis–trans isomerism represents one extreme of the general notion that a protein can exist in conformational substates. Two alternative conformations for the backbone of a hexapeptide segment (Thr45–Ile50) have been observed in crystals of the protein erabutoxin (Smith et al., 1986). These authors state that conformational heterogeneity is widespread in proteins and that it should be detectable in X-ray analyses at, or below, 2-Å resolution. Structural heterogeneity has also been observed for proteins in solution. For example, two alternatively folded states for the protein staphylococcal nuclease have been observed with ^1H NMR methods (Fox et al., 1986), and strong evidence has been presented which indicates

[4] A reviewer has raised an important concern over the interpretation of data from NOESY experiments acquired with a 200-ms mixing time. Based on our extensive studies of NOE buildup in wild-type and P43G r-calbindin (Kördel and Chazin, unpublished results), cross peaks in 200-ms spectra are observed for interproton distances up to approximately 5 Å, either directly or through a limited amount of spin diffusion. There is no adverse effect on the comparative, qualitative analyses presented here.

that the origin of this heterogeneity is proline cis–trans isomerism (Evans et al., 1987). Two conformations for the unfolded form of this protein have also been found (Evans et al., 1989). Our ^{1}H NMR studies have provided a direct characterization of the structural consequences of proline cis–trans isomerization in calbindin D_{9k}. It appears likely that multiple conformations of proteins are more common than reported so far. Our results show that the structural effect can be quite subtle and, therefore, suggest that great care may be needed to detect this phenomenon.

Due to the presence of two isoforms of r-calbindin in solution, evaluation of NOEs for structure calculations presents a serious problem. The main difficulty is the inability to distinguish the relative contributions from the two forms to the intensity of cross peaks, for those cases where corresponding cross peaks of the two forms are degenerate. Pro43 → Gly calbindin D_{9k} has been expressed and purified to circumvent this problem. This mutant has an identical distribution of secondary structure and global folding pattern, with minor and highly localized structural differences near the site of mutation. The differences in NMR parameters between the mutant and the major isoform of wild-type r-calbindin are smaller than those between the two isoforms of the wild-type protein. Characterization of the binding affinities and binding kinetics of the mutant protein by ^{43}Ca and ^{113}Cd NMR shows that the nature of the Ca^{2+} ligands is also highly similar to native calbindin D_{9k}. These results provide confidence in proceeding with the experiments and calculations necessary to produce high-resolution three-dimensional solution structures of Ca^{2+}-bound and Ca^{2+}-free P43G r-calbindin, toward our goal of characterizing the structural basis for the regulatory mechanism in the calmodulin family of calcium-binding proteins.

Acknowledgments

We thank Peter Brodin and Dr. Thomas Grundström for supplying protein pellets isolated from *Escherichia coli*, Eva Thulin for purification and preparation of the r-calbindin samples, Dr. Mark Rance for continued support with experimental methods, Dr. Nicholas Skelton for preparing Figure 7, Jerri Columpus for assistance in preparation of the manuscript, and reviewers for their helpful comments.

References

Babu, Y. S., Bugg, C. E., & Cook, W. J. (1988) *J. Mol. Biol. 204*, 191–204.

Billeter, M., Braun, W., & Wüthrich, K. (1982) *J. Mol. Biol. 155*, 321–346.

Brandts, J. F., & Lin, L.-N. (1986) *Methods Enzymol. 131*, 107–129.

Brodin, P., Grundström, T., Hofmann, T., Drakenberg, T., Thulin, E., & Forsén, S. (1986) *Biochemistry 25*, 5371–5377.

Brodin, P., Drakenberg, T., Thulin, E., Forsén, S., & Grundström, T. (1989) *Protein Eng. 2*, 353–358.

Chazin, W. J., Goldenberg, D. P., Creighton, T. E., & Wüthrich, K. (1985) *Eur. J. Biochem. 152*, 429–437.

Chazin, W. J., Rance, M., & Wright, P. E. (1988) *J. Mol. Biol. 202*, 603–622.

Chazin, W. J., Kördel, J., Drakenberg, T., Thulin, E., Brodin, P., Grundström, T., & Forsén, S. (1989a) *Proc. Natl. Acad. Sci. U.S.A. 86*, 2195–2198.

Chazin, W. J., Kördel, J., Drakenberg, T., Thulin, E., Hofmann, T., & Forsén, S. (1989b) *Biochemistry 28*, 8646–8653.

Davis, D. G. (1989) *J. Magn. Reson. 81*, 603–607.

Drakenberg, T., Forsén, S., & Lilja, H. (1983) *J. Magn. Reson. 53*, 412–422.

Drakenberg, T., Hofmann, T., & Chazin, W. J. (1989) *Biochemistry 28*, 5946–5954.

Evans, P. A., Dobson, C. M., Kautz, R. A., Hartfull, G., & Fox, R. O. (1987) *Nature 326*, 266–268.

Evans, P. A., Kautz, R. A., Fox, R. O., & Dobson, C. M. (1989) *Biochemistry 28*, 362–370.

Forsén, S., Linse, S., Thulin, E., Lindegård, B., Martin, S. R., Bayley, P. M., Brodin, P., & Grundström, T. (1988) *Eur. J. Biochem. 177*, 47–55.

Fox, R. O., Evans, P. A., & Dobson, C. M. (1986) *Nature 320*, 192–194.

Grathwohl, C., & Wüthrich, K. (1981) *Biopolymers 20*, 2623–2633.

Herzberg, O., & James, M. N. G. (1988) *J. Mol. Biol. 203*, 761–779.

Kördel, J., Forsén, S., & Chazin, W. J. (1989) *Biochemistry 28*, 7065–7074.

Kretsinger, R. H. (1987) *Cold Spring Harbor Symp. Quant. Biol. 52*, 499–510.

Linse, S., Brodin, P., Drakenberg, T., Thulin, E., Sellers, P., Elmdén, K., Grundström, T., & Forsén, S. (1987) *Biochemistry 26*, 6723–6735.

Linse, S., Brodin, P., Johansson, C., Thulin, E., Grundström, T., & Forsén, S. (1988) *Nature 335*, 651–652.

Macura, S., & Ernst, R. R. (1980) *Mol. Phys. 41*, 95–117.

Madison, E. L., Goldsmith, E. J., Gerard, R. D., Gething, M.-J. H., & Sambrook, J. F. (1989) *Nature 339*, 721–723.

Marion, D., & Wüthrich, K. (1983) *Biochem. Biophys. Res. Commun. 113*, 967–974.

Markley, J. L., Croll, D. H., Krishnamoorthi, R., Ortiz-Polo, G., Westler, W. M., Bogard, W. C., Jr., & Laskowski, M., Jr. (1986) *J. Cell. Biochem. 30*, 291–309.

McConnell, H. M. (1958) *J. Chem. Phys. 28*, 430–431.

Moews, P. C., & Kretsinger, R. H. (1975) *J. Mol. Biol. 91*, 201–228.

Pardi, A., Wagner, G., & Wüthrich, K. (1983) *Eur. J. Biochem. 137*, 445–454.

Pielak, G. J., Boyd, J., Moore, G. R., Williams, R. J. P. (1988) *Eur. J. Biochem. 177*, 166–177.

Ringe, D. (1989) *Nature 339*, 658–659.

Satyshur, K. A., Rao, S. T., Pyzalska, D., Drendel, W., Greaser, M., & Sundaralingam, M. (1988) *J. Biol. Chem. 263*, 1628–1647.

Smith, J. L., Hendrickson, W. A., Honzatko, R. B., & Sheriff, S. (1986) *Biochemistry 25*, 5018–5027.

Stassinopoulou, C. I., Wagner, G., & Wüthrich, K. (1984) *Eur. J. Biochem. 145*, 423–430.

Szebenyi, D. M. E., & Moffat, K. (1986) *J. Biol. Chem. 261*, 8761–8777.

Tsai, M.-D., Drakenberg, T., Thulin, E., & Forsén, S. (1987) *Biochemistry 26*, 3635–3643.

Vogel, H. J., & Forsén, S. (1987) in *Biological Magnetic Resonance* (Berliner, L. J., & Reuben, J., Eds.) Vol. 7, pp 249–309, Plenum, New York.

Wagner, G. (1983) *J. Magn. Reson. 55*, 151–156.

Wagner, G., Tschesche, H., & Wüthrich, K. (1979) *Eur. J. Biochem. 95*, 239–248.

Wendt, B., Hofmann, T., Martin, S. T., Bayley, P., Brodin, P., Grundström, T., Thulin, E., Linse, S., & Forsén, S. (1988) *Eur. J. Biochem. 175*, 439–445.

Wüthrich, K. (1989) *Science 243*, 45–50.